

## Article

# Shallow Seismic Refraction Tomography Images from the Pieniny Klippen Belt (Southern Poland)

Kamil Cichostępski , Jerzy Dec , Jan Golonka \* and Anna Waśkowska 

Faculty of Geology, Geophysics and Environmental Protection, AGH University of Krakow, al. A. Mickiewicza 30, 30-059 Krakow, Poland; geodec@agh.edu.pl (J.D.); waskowsk@agh.edu.pl (A.W.)

\* Correspondence: kcichy@agh.edu.pl (K.C.); jgonlonka@agh.edu.pl (J.G.)

**Abstract:** The Pieniny Klippen Belt (PKB) is located between the Central and the Outer (Flysch) Carpathians and forms a narrow zone with a complex structure, often described as a *mélange*. It is composed of numerous tectonic elements of different size including strike-slip-bounded tectonic blocks, thrust units, toe thrusts and olistostromes combined together and representing different lithologies. To aid the geological interpretation of the *mélanges* of the PKB in the Spiskie Pieniny Mountain Region (South Poland), seismic refraction tomography was conducted. Isolated limestone outcrops consist of Jurassic limestones that stand out in the landscape. They form the horizontal narrow belt. In this belt, limestone olistoliths are surrounded by a matrix consisting of sandstones, mudstones and marl sequences forming a sedimentary *mélange*. The seismic refraction tomography measurements conducted along three profiles across this belt showed significant horizontal and vertical seismic velocity variations, which revealed the complex geological structure of this area. The Złatne, Branisko and Hulina Units were distinguished within the PKB structure. The high-velocity objects detected within the Hulina Unit were found to correspond to limestone outcrops and form isolated blocks surrounded by flysch deposits representing a chaotic sedimentary complex.

**Keywords:** Central Carpathians; Pieniny Klippen Belt; seismic refraction tomography; flysch; *mélange*



**Citation:** Cichostępski, K.; Dec, J.; Golonka, J.; Waśkowska, A. Shallow Seismic Refraction Tomography Images from the Pieniny Klippen Belt (Southern Poland). *Minerals* **2024**, *14*, 155. <https://doi.org/10.3390/min14020155>

Academic Editor: Manuel Francisco Pereira

Received: 23 December 2023

Revised: 27 January 2024

Accepted: 29 January 2024

Published: 31 January 2024



**Copyright:** © 2024 by the authors. Licensee MDPI, Basel, Switzerland. This article is an open access article distributed under the terms and conditions of the Creative Commons Attribution (CC BY) license (<https://creativecommons.org/licenses/by/4.0/>).

## 1. Introduction

The most northern fragments of the European Alpides [1] are located in several countries, including Southern Poland (Figure 1). From north to south, the main structural units are the North European Platform, the Miocene Carpathian Foredeep, the Outer Flysch Carpathians and the Central Western Carpathians. The Pieniny Klippen Belt zone separates the Outer Flysch Carpathians from the Central Western Carpathians [2–5]. The Pieniny Klippen Belt (PKB) was identified by [6] as a separate geological unit. It is a suture zone that consists of stratigraphical, lithological and tectonic elements—thrusts as well as olistostromes—with different age and characteristics [2–5]. They are mixed together, forming a chaotic structure, in the PKB, which is referred to as a *mélange* [7–9]. Its formation was due to both tectonic and sedimentary processes. The elements of this *mélange*, consisting of Mesozoic limestone blocks, are characteristic morphological elements of the PKB [5]. They are harder than the surrounding rocks, which consist of other sedimentary, mainly clastic, deposits like sandstones, mudstones and marls. The Mesozoic limestones and associated rocks were studied by geologists from Austria, Slovakia and Poland [6,10–14]. These studies allowed distinguishing several successions based on lithological differences. Additional successions were distinguished based on Upper Cretaceous–Paleogene flysch sequences [15]. Great resistance to erosion spurred the separation of limestone blocks in morphology, producing rocky formations along the PKB stretch [5]. The current relief of the PKB depends on its complex structure and on weathering processes, which expose the limestone elements by removing other less competent clastic deposits. The presence of

these limestone rocky forms along the narrow structure distinguishes the landscape of the PKB and is also reflected in the name of the unit, since the term “Klippen Belt” originates from the word cliff (Klippen, in German) [6]. “Pieniny” is a geographic term. It identifies the mountain range along Poland and Slovakia, part of the PKB that stretches from Austria to Romania, with numerous “Klippen” [5] (Figures 2a and 3). These cliffs form harder, more erosion-resistant elements, residing within less competent clastic deposits, like sandstones, shales and marls that form turbiditic (flysch) complexes. The limestone blocks have mainly an olistolith origin, and slipped down from shallower zones to the deeper basinal areas.

The limestone cliffs are concentrated in two olistostrome belts [5]. The older one derived from the subduction of the southern Alpine Tethys, while the other formed from the shift of the accretionary wedge to the north. The other cliffs, as well as the whole flower structure of the PKB, formed as a result of tectonic deformational processes. They are an effect of the collision and strike-slip movement of the lithospheric plates [1–5]. The PKB flower structure is separated in the north and south by deep-rooted faults and is related to the diapiric mélange in the Pieniny Mountains in Poland.

The study of this mélange is key for the description of the PKB regional geology, paleogeography and evolution. The PKB structure is controversial. Geologists working in different areas of the PKB have different, equally divergent opinions about the PKB structure [3–5,16–21]. Learning about the structure of the PKB and reconstructing from it the sequence of past geological processes requires further detailed study of its various elements. To facilitate the geological interpretation of the mélanges of the PKB, the authors conducted shallow seismic refraction tomography, which allows mapping subsurface geological features with high accuracy.

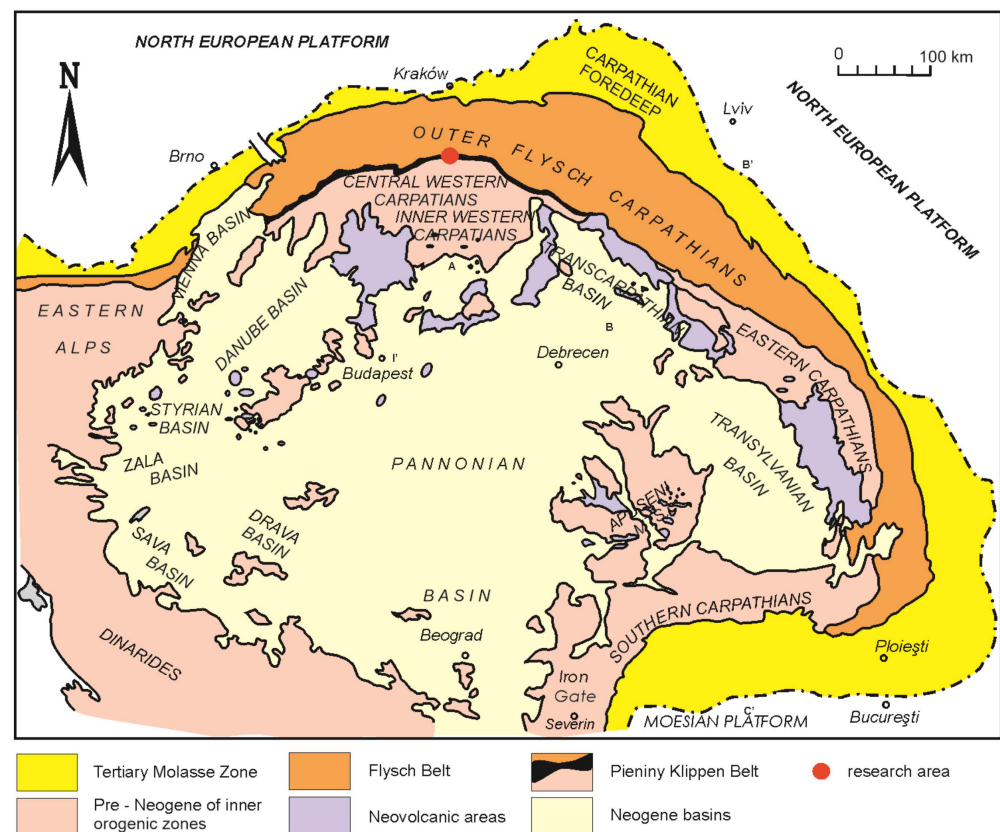


**Figure 1.** Location of the research (see Figure 2a) area on a geological sketch map of the Carpathians and adjacent areas. After [22], modified.



Seismic refraction tomography (SRT) is a geophysical technique that allows the determination of the geological and geotechnical characteristics of the subsurface for environmental and engineering studies [23]. It allows the recognition of the distribution of individual units present in subsurface structures and is non-invasive. The goal of SRT surveys is to obtain a 2D seismic wave velocity model of the subsurface. Seismic refraction tomography was widely employed in the late 1980s and early 1990s, mainly for the investigation of deep crustal structures [24]. Over time, seismic refraction was adapted for near-surface geophysics, and seismic reflection profiling has become the main method for deeper investigations [25–27]. Today, SRT is an established near-surface investigation method used in environmental and engineering studies [28]. Seismic refraction tomography performs well in many situations where traditional seismic refraction methods fail, such as in the presence of velocity structures with both lateral and vertical velocity gradients [29,30]. SRT is commonly applied for, e.g., bedrock mapping [31–33], groundwater level determination [34,35], the characterization of landslide geometry [36,37], the assessment of rippability [38,39] and seepage detection [40].

SRT measurements were carried out along survey lines that were oriented perpendicularly to the general strike of the PKB, especially to the belt of limestone outcrops, which is one of the most spectacular features in the investigated part of the PKB, well visible as small hills built of Jurassic and Cretaceous rocks. The purpose of this research was to determine the geological structure of the area in detail.

## 2. Study Area and Geological Setting

The study area is located in the Spisz (Spiskie) Pieniny Mountain Region, in Southern Poland, in a region with several limestone blocks, including the popular Obłazowa-Kramnica, Lorencowe Skałki and Korowa Skałka, which stand out from the uniform morphology of the area (Figure 3). The Central Carpathians and the PKB are located in this region [1–5,41]. The Central Carpathian rocks crop out in the southernmost part of the studied area. They consist of Central Carpathian Paleogene flysch deposits (Podhale Flysch), mainly made of Eocene sandstone and shales of the Szaflary Formation [20,21] (Figure 3). The subvertical fault marks the boundary between the Central Carpathian Paleogene deposits and the PKB [5,41]. The Central Carpathian Paleogene deposits are strongly deformed. At the contact with the PKB, they fall steeply (70–90°), but a few kilometers south of the PKB they fall gently (0–45°) [5,21].

The PKB rocks were deposited during Jurassic–Neogene times (Figure 2b) in two basins—Złatne and Magura—separated by the Czorsztyn Ridge [5,15,21] (Figure 4). The Jurassic–Lower Cretaceous deposits consist mainly of limestone and radiolarite [14,41]. They are divided by several successions, depending on their paleogeographic position within ridge, slope and deeper basin. The Zawiasy and Hulina Successions were deposited on the northern slope of the Czorsztyn Ridge; the Pieniny, Branisko, Czestezik and Niedzica Successions were deposited on the southern slope of the basin. The Coresztyn Succession was deposited in the central part of this ridge. Albian–Neogene rocks consist mainly of flysch and marls deposited during the formation of an accretionary prism [5,14,41]. The rocks of the Czorsztyn Succession are olistoliths redeposited into the mélangé (Figure 3) formed in the southeastern part of the Magura Basin [5]. The current structure of the PKB is the result of compressional and transpressional movements [5,21]. The compressional deformations produced thrust sheets (nappes). Three structural units (nappes) were distinguished within the investigated area (Figure 3). The southern Złatne Nappe is located north of the Central Carpathian Paleogene flysch. It mainly consists of Upper Cretaceous flysch of the Sromowce Formation [5,21]. The northern Hulina Nappe is built mainly of Upper Cretaceous–Paleogene flysch of the Jarmuta and Malinowa formations [5,14,21,41]. Complexes with prevailing thick-bedded massive sandstones and complexes with an equal mixture of shales and sandstones can be distinguished within this flysch. Also, a block-in-matrix zone with olistoliths forming a sedimentary mélangé can be distinguished within the Hulina Nappe, north of the boundary with the Złatne Nappe (Figure 3). This zone

corresponds to a belt of limestone outcrops. The olistoliths are mainly composed of Jurassic–Cretaceous limestones belonging to the Czorsztyn Succession. They are often arranged vertically, in contrast to the 45-degree-dipping flysch nappes [21]. Locally, between the Złatne and the Hulina nappes, there is the Branisko Nappe, built mainly of Jurassic–Lower Cretaceous limestone and radiolarite (Figure 3).

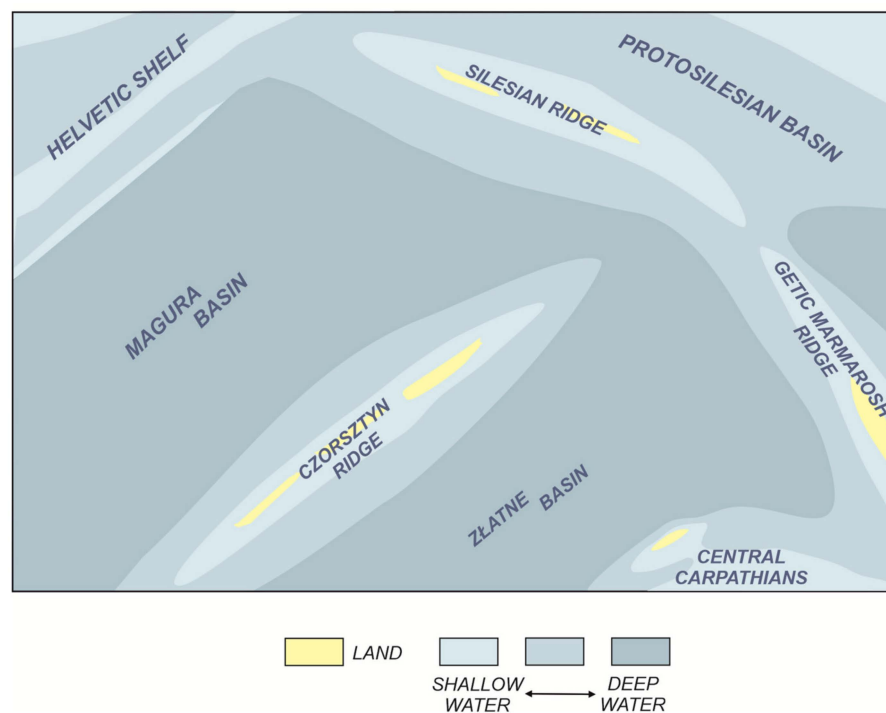


**Figure 4.** Paleogeography of the Alpine Tethys (Magura Basin, Czorsztyn Ridge and Złatne Basin) during the Albian (112 Ma). Modified from [5].

### 3. Methods

Seismic refraction tomography utilizes artificially generated seismic waves that propagate through a subsurface. The speed of propagation of seismic waves varies and is dependent on the individual parameters of the medium, including the type of lithology, its textural and structural features and the presence of tectonic structures [42]. According to geotechnics, an increase in seismic wave velocity indicates a more solid material [43]. The achievement of a lithological inventory of the studied area, together with the knowledge of parameters such as the speed of propagation of seismic velocity in different media offers the possibility to determine the internal structure of a subsurface, analyzing the thickness of soil and weathered layer and the lithological distribution in the internal structures.

Seismic refraction tomography is based on the arrival times of seismic waves that were critically refracted at the interface between layers having different velocity. The travel times of the seismic waves are recorded by receivers (geophones) placed in a line. Based on multiple registrations using a combination of shot points and geophones, a collection of travel times can be obtained. The inversion of those travel times allows obtaining a velocity model of the subsurface [44]. The depth of investigation can be from 0.3 to 0.5 times the receiver spread, but depends on the geology beneath the spread. The gridded inversion technique determines the velocity of individual 2-dimension blocks within a profile as opposed to modeling velocities as layers. As a result, SRT provides good resolution of the complex velocity structure of a subsurface [29]. However, velocity reversal or hidden layers can cause errors in tomographic calculations. Velocity reversal occurs when a layer has a lower seismic velocity than an overlaying layer. In such a situation, the refraction wave is not created. Another limitation is due to blind zones, which occur where there is insufficient velocity contrast or thickness difference between layers.

#### 4. Seismic Refraction Tomography Measurements

The seismic acquisition set-up was deployed along three profiles: S01, S02 and S03. The survey lines passed through the belt of the limestone outcrops zone and extended far enough into its surrounding formations on both the north and the south sides (Figure 5). They covered the PKB structure and its surrounding areas. Figure 6 shows a view of a belt of limestone outcrops and the nearby geophysical profile S03.

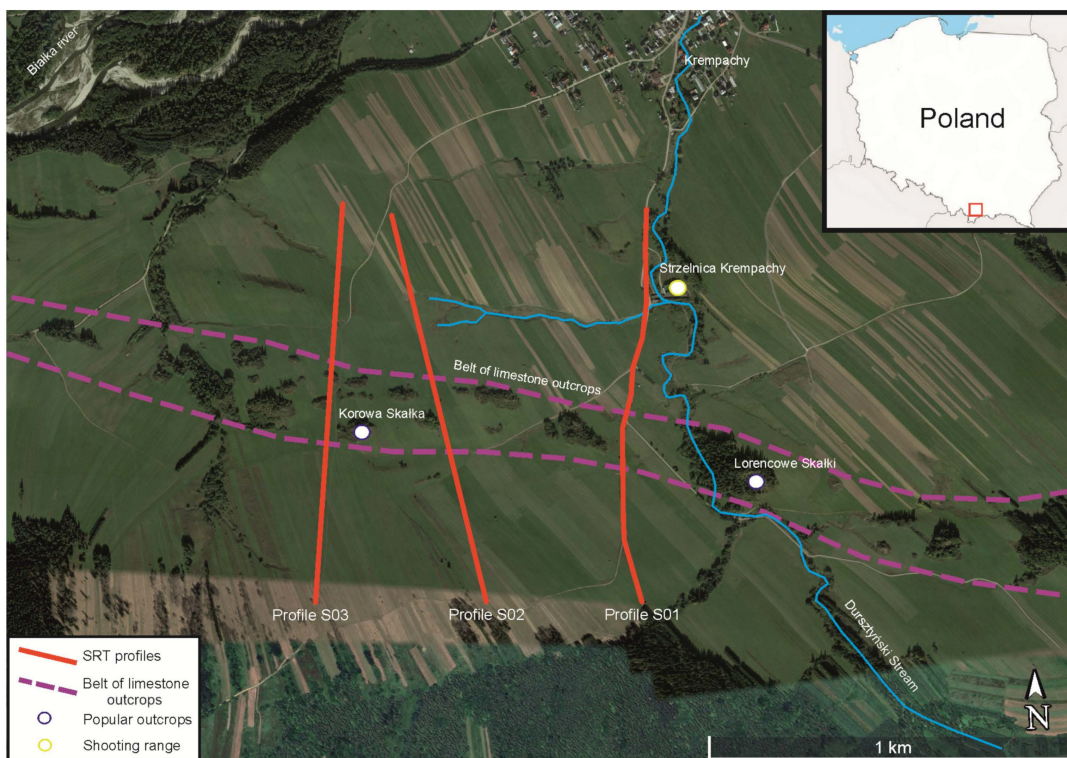


Figure 5. Location of the seismic refraction tomography measurements.

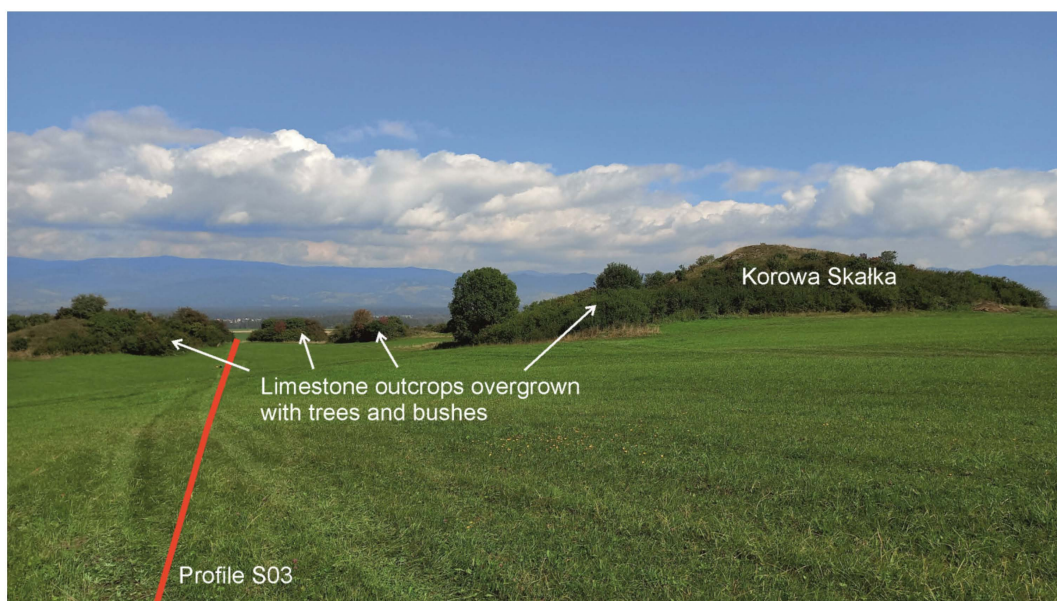
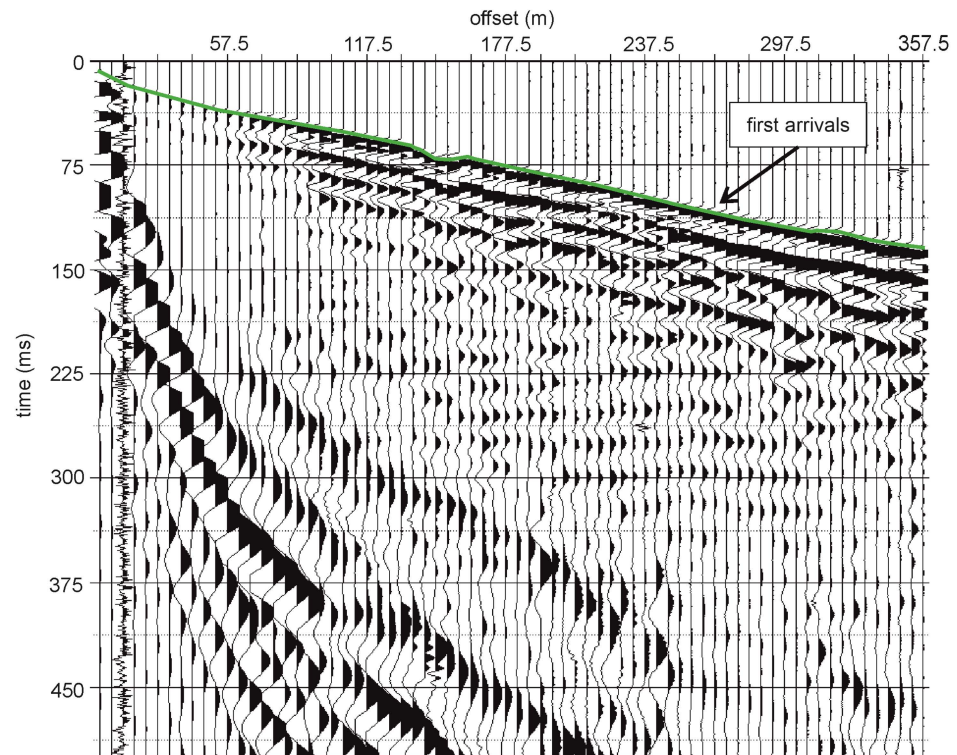


Figure 6. Illustrative photo of a view from the south of a fragment of the S03 profile (from ca. 390 m to 625 m) and the surrounding limestone outcrops. The top of the Korowa Skalka outcrop is approximately 13 m above the ground surface.

The data were collected using three Geometrics Geodes with 14 Hz vertical geophones spaced 5 m apart. The active spread consisted of 72 geophones, which corresponded to a length of 355 m. The spread spanned over 1075 m and was measured in three parts with overlaps of 115 m (roll-along technique). As a seismic source, we used Gisco ESS-500 Turbo (accelerated weight drop of 227 kg—impact velocity of 6 m/s, with energy of 4088 J). The first shot's location was one-half the distance of the receiver from the first geophone, and the shots were located 30 m apart. To obtain a high signal-to-noise ratio, typically, up to three weight drops were performed at each shot position. Then, the corresponding records were vertically stacked. The sampling rate was 0.5 ms, and the recording time was 1 s. The acquired data had excellent quality with clear first arrivals (Figure 7).



**Figure 7.** Exemplary P-wave shot gather from the beginning of the S01 profile. The gather shows a high S/N ratio, with first breaks (green line) clearly visible even at a long distance from the seismic source position (offset).

The obtained seismic data were processed in ZondST2D software ver. 6.0 (Zond Software Ltd., Paphos, Republic of Cyprus). The times of the first P-wave arrivals in each shot gather were manually picked. A P-wave velocity model was derived from the collection of those travel times by using the tomographic inversion method. This method utilizes an initial velocity model and iteratively traces rays through the model, comparing the calculated travel times to the measured travel times, modifying the model and repeating the process until the difference between the calculated and the measured travel times of the first arrivals is minimized [29,44,45]. The initial model for the inversion was built using a smooth gradient velocity distribution in relation to depth. The parameters of the model varied from 0.5 km/s to 5 km/s. The inversion process was stopped after 10 iterations, reaching an RMS (root-mean-square) error of 1.3%. The final velocity models (Figure 8) were trimmed in the areas where there was no ray coverage. With the applied methodology, the maximum depth of subsurface seismic imaging was 90 m.

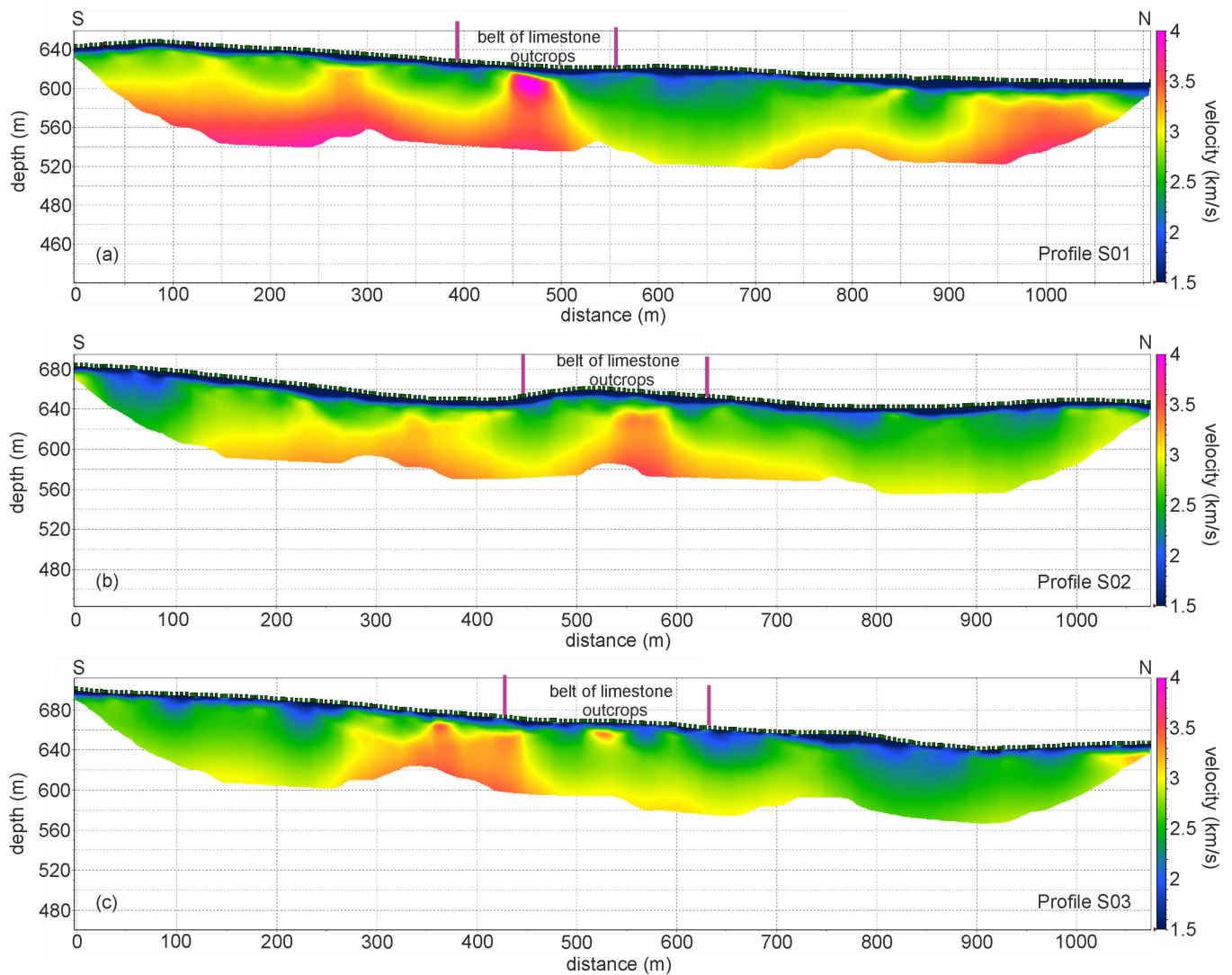


**Figure 8.** The results of seismic refraction tomography. (a) Profile S01, (b) profile S02, (c) profile S03. The purple lines indicate the area of the belt of limestone outcrops on the surface.

## 5. Results and Interpretation

Seismic velocity identifies rocks and their condition. Low velocities may indicate the presence of soft rocks like mudstones, marls and soil, while high velocities may indicate a solid rock. The more weathered the rocks are, the greater the impact on their seismic characteristics, and the lower the velocity [46,47]. The SRT cross sections obtained for the Pieniny Spiskie Mountains showed significant horizontal and vertical seismic velocity variations. The velocity ranged from 1.5 km/s to 4.5 km/s, showing strong lateral contrasts in the subsurface properties. This revealed the complex geological structure of the study area (Figure 8).

For the proper interpretation of the obtained results, we used geological maps of the region (Figures 2 and 3) and performed geological observations of outcrops and along the Dursztyński stream section (Figure 9, for the stream location, see Figure 3). This allowed for a correlation of the velocity distribution with the rock type (Figure 10).

According to the geological maps and the field study, we found that thin-bedded sandstones and mudstones are component of the flysch sequences of the Central Carpathian Paleogene, Złatne and Hulina units, limestones are typical of the Branisko Unit, and thick-bedded sandstones are characteristic of the Jarmuta Formation of the Hulina Unit.



**Figure 9.** Illustrative photos of examples of mélangé deposits along the Dursztyński stream. (a) Olistolith of Jurassic limestone, (b) Upper Cretaceous marly deposits hosting olistoliths. The height of the visible olistolith in (a) is about 2 m.

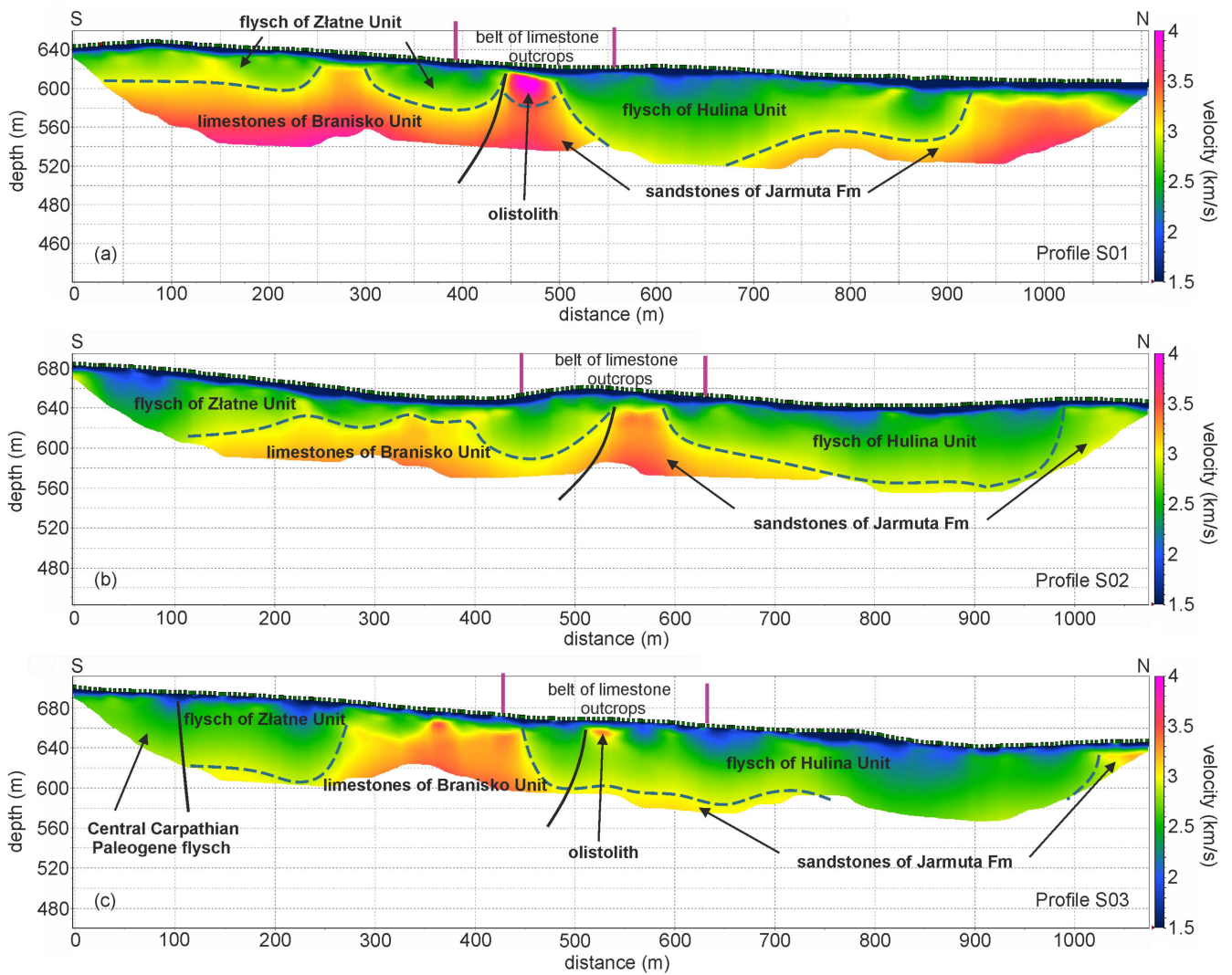


**Figure 10.** The geological interpretation of seismic refraction tomography. (a) Profile S01, (b) profile S02, (c) profile S03. The purple lines indicate the area of the belt of limestone outcrops. Dashed lines—interpreted boundaries between geological units. Black lines—faults.

The lowest velocities (up to 1.5 m/s, marked in dark blue) corresponded to soil, which is the first outer layer, with a thickness of about 2 m. At a shallow depth, bedrock with high variation in velocity was found. A relatively higher seismic velocity (light blue and green colors) indicated the presence of flysch. Velocities up to 2.7 km/s (marked in light blue and green) corresponded to flysch dominated by mudstone or marl, while higher velocities (up to 3 km/s, marked in yellow) indicated that the main component was sandstones. The highest velocities (orange and purple colors) corresponded to limestone or massive sandstone. Velocity values from 1.6 to 2.7 km/s were interpreted as flysch deposits of the Central Carpathian Paleogene, Złatne and Hulina Units, while higher velocities (from 3.2 to 4.5 km/s) were interpreted as both limestone and sandstone (Branisko Unit and Jarmuta Formation). The velocities depended on the degree of weathering and the mineral composition of the rocks and varied within certain ranges of values.

The profile S01 (Figure 10a) from the south presented first relatively low-velocity flysch of the Złatne Unit with a thickness of about 40 m. High-velocity limestones of the Branisko Unit were identified below. Those units were found to span the first 450 m of the profile, bounded by the high-velocity sandstones of the Jarmuta Formation. This boundary appeared to be below the belt of limestone outcrops. The massive sandstones of the Jarmuta Formation dipped towards the north and then slowly emerged towards the surface, starting from the 700th meter of the profile. Their outcrops are exposed near the “Strzelnica Krempachy” shooting range (see Figure 3). The Jarmuta Formation is covered by flysch deposits belonging to the Hulina Unit.

A similar velocity distribution was found for the S02 profile (Figure 10b), which first showed flysch of the Złatne Units, lying on the limestones of the Branisko Unit. The thickness of the Złatne Unit was found to vary from 20 to 80 m. The boundary between these units and the sandstones of the Jarmuta Formation was marked at the 550th meter of the profile. The sandstones dipped toward the north and appeared covered by flysch of the Hulina Unit, which reached a thickness up to 80 m. At the 980th meter of the profile, they started to emerge towards the surface. The velocities of the Jarmuta sandstones were lower compared to those in the profile S01, which may indicate that they are more weathered.

The S03 profile started at the southernmost point (Figures 5 and 10c). It first showed low-velocity Central Carpathian Paleogene flysch, spanning the first 100 m of the profile. There is an almost vertical fault that limits the Pieniny Klippen Belt from the south [21]. The low-velocity Złatne Unit was identified between 100 and 280 m of the profile. Below, at the depth of 65 m, high-velocity limestones of the Branisko Unit were identified. At the 280th meter of the profile, they suddenly emerged close to the surface. This zone spanned 450 m of the profile, where, once again, low-velocity shales and thin sandstones of the Złatne Unit were found, and limestone of the Branisko Unit dipped steeply below the depth range of the refraction tomographer. At the 510th meter of the profile, a contact between low-velocity flysch of the Złatne and Hulina Units could be observed. Jarmuta high-velocity sandstones were found at depths below 80 m, where they dipped toward the north and then, after the 1000th meter of the profile, suddenly emerged close to the surface.

An interesting rounded, isolated object with very high velocity was seen at the 475th m of the S01 profile, at the tectonic boundary between the Złatne Unit, the Branisko Unit and the Jarmuta Formation (Figure 10a). It appeared located within the belt of limestone outcrops. At the same place on the surface, just a few meters from the profile, there is an outcrop of limestone. This coincidence allowed us to identify the object as limestone, probably an olistolith embedded in sandstone. A similar contact could be observed near the Lorencowe Skałki limestone block (for its location, see Figure 5) where limestone lies directly on sandstone. Such contact could be observed in a nearby stream. The same situation was found at the 525th m of the S03 profile, where an object with very high velocity, corresponding to a limestone outcrop near the profile was observed. There was no similar isolated object in the S02 profile, only a high-velocity block that corresponded to sandstone of the Jarmuta Formation. One possible cause of this situation can be that some of the limestone outcrops within the belt of limestone outcrops are uneroded blocks of

the Branisko Unit, while others are rock fragments what detached from the Branisko Unit. Those objects may be interpreted as tectonic mélanges. They are the result of thrusting that had an impact in fault or shear zones, but also of mass rocks displacement.

Geological observations carried out in the southern part of the Dursztyński stream allowed us to differentiate the complexes of south-dipping Upper Cretaceous thin-bedded turbiditic sandstones and shales of the Sromowce Formation, as well as the almost vertical Eocene thin- and medium-bedded turbiditic sandstones and shales of the Szaflary Formation. This chaotic complex of limestones, marls, mudstones and sandstones is located north of the flysch complex of the Sromowce Formation. The Jurassic crinoid and nodular limestones, as well as the Upper Cretaceous marls (Jaworki Marls Formation) belong to the Czorsztyn Succession of the Pieniny Klippen Belt. The complexes of calcareous Maastrichtian–Paleocene turbiditic sandstone of the Jarmuta Formation and variegated, mostly red, hemipelagic mudstones (with intercalations of thin-bedded turbiditic sandstones) of the Malinowa Shale are present in the northern part of the Dursztyński stream section.

## 6. Discussion

The combination of geologic cartography and geophysical methods made it possible to determine the distribution of the tectonic and sedimentary elements of mélanges in the PKB. The southern part of the analyzed geophysical profiles appeared as a turbiditic succession composed of sandstones and mudstones. We found that higher velocity rock complexes constitute a sandstone-dominated flysch, where areas of low-velocity rocks show prevailing claystones and mudstones. Flysch characterized both the Central Carpathian Paleogene deposits and the Złatne Unit. It was not possible to distinguish this boundary using only seismic data due to the similar physical parameters of the rocks occurring in the two units. This boundary is outcropped in the Dursztyński stream section and was extrapolated into the seismic profiles. It represents the upper part of the Southern Pieniny Fault, the subvertical major tectonic boundary separating the Central Carpathians from the Pieniny Klippen Belt. This fault is well visible in deep seismic profiles [17,21]. It is part of the flower structure, originated during the strike-slip motion of the Central Carpathian and North European plates [3,4,21,41].

The low-velocity flysch of the Złatne Unit was found to overlay the high-velocity limestone complex. Extrapolation from the nearby Branisko Mountain in the Spisz Pieniny Mountains suggests interpreting this complex as Jurassic–Lower Cretaceous pelagic cherty limestones (Pieniny Limestone Formation) of the Branisko Unit. The belt of limestone outcrops is separated from the Złatne Unit by a tectonic boundary. This belt was found to be a chaotic sedimentary complex containing limestones, marls, sandstones and mudstones. It represents an olistostrome belonging to the Hulina Unit. Low-velocity complexes of hemipelagic mudstones with intercalations of thin-bedded sandstones were identified in the Malinowa Shale Formation deposited within the Magura Basin. The northernmost part of the geophysical profiles identified high-velocity rock complexes. After correlation with the geological cartography data, these high-velocity complexes appeared to correspond to the massive thick-bedded sandstones of the Jarmuta Formation belonging to the Hulina Unit.

The nature of geophysical measurements and their dependence on many equal factors make them not always clear and unambiguous. For example, changes in vertical or lateral velocity can be interpreted as changes in lithology or as weathering zones. The interpretation of data using one method has limits. Reliability can be improved by applying additional geophysical surveys using other methods [5,48] and obtaining data from a maximally large database of geological data from surface and subsurface structures, such as boreholes. The use of specific methods, whose implementation has both advantages and disadvantages, must be analyzed in detail, and the choice of the method should depend on the type of information to be obtained, the specifics of the area and the experience of the geophysicists performing the survey.

There are not many shallow geophysical studies regarding the Pieniny Klippen Belt in the literature [5]. Most studies focused on the geological interpretation of the deep structure of PKB [21,49–51] or on measuring seismicity and investigating faults in the area, because the PKB is tectonically active [26,52,53]. To obtain a more detailed and unambiguous image of the shallow part of the PKB area, the next step in our research will be to perform more seismic refraction tomography measurements, followed by electrical resistivity tomography and gravimetric surveys.

## 7. Conclusions

SRT cross sections across the Pieniny Klippen Belt in the Pieniny Spiskie Mountains (Krempachy area) showed significant horizontal and vertical seismic velocity variations. Low-velocity complexes were found to correspond to flysch deposits dominated by mudstones and marls as well as claystone- and clay-dominated weathering deposits or soils. High velocities were related to the presence of limestones or massive sandstones. In the SRT cross sections, the tectonic Złatne, Branisko and Hulina Units were distinguished within the PKB. The deposits of the Hulina Unit representing the northern part of the PKB appeared to consist of three lithological complexes: mudstones, marls and thick-bedded sandstones. The northern part of the Hulina Unit was found to be dominated by a sedimentary *mélange* containing isolated limestone blocks interpreted as olistoliths, which form the "Klippen". The Branisko Unit is located in the southern part of the PKB, which appeared mostly covered by flysch deposits of the Złatne Unit. The subvertical fault, which is the contact structure of the PKB with the adjacent part of the Central Carpathians, was not clearly visible in the SRT cross sections because the rocks on both fault sides displayed similar physical parameters. The fault location was derived from the geological cartography (Figure 3).

**Author Contributions:** Conceptualization, K.C. and J.G.; methodology, K.C. and J.D.; software, K.C.; validation, J.D., J.G. and A.W.; formal analysis, J.G.; investigation, K.C., J.D., J.G. and A.W.; writing—original draft preparation, K.C.; writing—review and editing, J.G.; supervision, J.D. and A.W.; project administration, J.D.; funding acquisition, J.G. All authors have read and agreed to the published version of the manuscript.

**Funding:** This research was financially supported by the Polish National Science Center, grant NCN no. 2019/35/B/ST10/00241, and by the AGH University of Krakow, subsidy fund no. 16.16.140.315.

**Data Availability Statement:** Data are contained within the article.

**Acknowledgments:** The authors would like to express appreciation to three anonymous reviewers for providing valuable comments and feedback on the manuscript.

**Conflicts of Interest:** The authors declare no conflicts of interest.

## References

1. Froitzheim, N.; Plašienka, D.; Schuster, R. Alpine tectonics of the Alps and Western Carpathians. In *The Geology of Central Europe. Volume 2: Mesozoic and Cenozoic*; McCann, T., Ed.; Geological Society: London, UK, 2008; pp. 1141–1232. [[CrossRef](#)]
2. Książkiewicz, M. Tectonics of the Carpathians. In *Geology of Poland. Vol. IV. Tectonics*; Pożaryski, W., Ed.; Wydawnictwa Geologiczne: Warszawa, Poland, 1977; pp. 476–604.
3. Birkenmajer, K. Geology of the Pieniny Klippen Belt of Poland. *Jahrb. Der. Geol. Bundesanst.* **1960**, *103*, 1–36.
4. Birkenmajer, K. Stages of structural evolution of the Pieniny Klippen Belt. *Carpathians. Stud. Geol. Pol.* **1986**, *88*, 7–32.
5. Golonka, J.; Waśkowska, A.; Cichostępski, K.; Dec, J.; Pietsch, K.; Łój, M.; Bania, G.; Mościcki, W.J.; Porzucek, S. *Mélange, Flysch and Cliffs in the Pieniny Klippen Belt (Poland): An Overview.* *Minerals* **2022**, *12*, 1149. [[CrossRef](#)]
6. Neumayr, M. Jurastudien. 3. Der Penninische Klippenzug. *Jb. Geol. Reichsan* **1871**, *21*, 451–536.
7. Greenly, E. *The Geology of Anglesey: Memoirs of Geological Survey. Vols I and II*; HM Stationary Office: London, UK, 1919; pp. 390–980.
8. Hsü, K.J. Principles of *mélanges* and their bearing on the Franciscan-Knoxville paradox. *Geol. Soc. Am. Bull.* **1968**, *79*, 1063–1074. [[CrossRef](#)]
9. Festa, A.; Dilek, Y.; Pini, G.; Codegone, G.; Ogata, K. Mechanisms and processes of stratal disruption and mixing in the development of *mélanges* and broken formations: Redefining and classifying *mélanges*. *Tectonophysics* **2012**, *568*, 7–24. [[CrossRef](#)]
10. Uhlig, V. Ergebnisse geologischer Aufnahmen in der westgalizischen Karpathen. Teil II. Der pienische Klippenzug. *Jahrb. Geol. Reichsanst.* **1890**, *40*, 559–824.

11. Andrusov, D. *Geologie der Tschechoslowakischen Karpaten II*; Akademie Verlag: Berlin, Germany, 1965; pp. 1–443.
12. Mišík, M. The Slovak part of the Pieniny Klippen Belt after the pioneering works of D. Andrusov. *Geol. Carpathica* **1997**, *48*, 209–220.
13. Horwitz, L.; Rabowski, F. Przewodnik do wycieczki Polskiego Towarzystwa Geologicznego w Pieniny (18–21.V.1929). *Rocz. Pol. Tow. Geol.* **1930**, *6*, 109–155.
14. Birkenmajer, K. Jurassic and Cretaceous lithostratigraphic units of the Pieniny Klippen Belt, Carpathians, Poland. *Stud. Geol. Pol.* **1977**, *45*, 1–158.
15. Sikora, W. Esquisse de la tectogénèse de la zone des Klippes des Pieniny en Pologne d’après de nouvelles données géologiques. *Rocz. Pol. Tow. Geol.* **1971**, *4*, 221–239.
16. Nemčok, J. Non-traditional view of East-Slovakian Klippen Belt. *Geol. Zb. Geol. Carpathicac* **1980**, *31*, 563–568.
17. Plašienka, D.; Michalík, J.; Soták, J.; Aubrech, R. Discussion of “Olistostromes of the Pieniny Klippen Belt, Northern Carpathians”. *Geol. Mag.* **2017**, *154*, 187–192. [[CrossRef](#)]
18. Jurewicz, E.; Segit, T.; Plašienka, D.; Chrapkiewicz, K. Discussion of “Seismic imaging of mélanges—Pieniny Klippen Belt case study”. *J. Geol. Soc.* **2021**, *178*, 629–646. [[CrossRef](#)]
19. Marzec, P.; Golonka, J.; Pietsch, K.; Kasperska, M.; Dec, J.; Cichostępski, K.; Lasocki, S. Reply to Discussion of ‘Seismic imaging of mélanges; Pieniny Klippen Belt case study’. *J. Geol. Soc.* **2021**, *178*, 2020–2111. [[CrossRef](#)]
20. Ludwiniak, M. Multi-stage development of the joint network in the flysch rocks of western Podhale (Inner Western Carpathians, Poland). *Acta Geol. Pol.* **2010**, *60*, 283–316.
21. Golonka, J.; Pietsch, K.; Marzec, P.; Kasperska, M.; Dec, J.; Cichostępski, K.; Lasocki, S. Deep structure of the Pieniny Klippen Belt in Poland. *Swiss J. Geosci.* **2019**, *112*, 475–506. [[CrossRef](#)]
22. Kováč, M.; Nagymarosy, A.; Oszczypko, N.; Ślaczka, A.; Csontos, L.; Marunteanu, M.; Matenco, L.; Márton, M. Palinspastic reconstruction of the Carpathian-Pannonian region during the Miocene. In *Geodynamic Development of the Western Carpathians. Geological Survey of Slovak Republic*; Rakús, M., Ed.; Dionýz Štúr Publishers: Bratislava, Slovakia, 1998; pp. 189–217.
23. Yilmaz, Ö. *Engineering Seismology with Applications to Geotechnical Engineering*; Society of Exploration Geophysicists: Tulsa, OK, USA, 2015.
24. Guterch, A.; Grad, M.; Špičák, A.; Brückl, E.; Hegedüs, E.; Keller, G.; Thybo, H. Special Contribution: An Overview of Recent Seismic Refraction Experiments in Central Europe. *Stud. Geophys. Geod.* **2003**, *47*, 651–657. [[CrossRef](#)]
25. Cichostępski, K.; Kwietniak, A.; Dec, J.; Kasperska, M.; Pietsch, K. Integrated geophysical data for sweet spot identification in Baltic Basin, Poland. *Ann. Soc. Geol. Pol.* **2019**, *89*, 215–231. [[CrossRef](#)]
26. Białoń, W.; Lizurek, G.; Dec, J.; Cichostępski, K.; Pietsch, K. Relocation of Seismic Events and Validation of Moment Tensor Inversion for SENTINELS Local Seismic Network. *Pure Appl. Geophys.* **2019**, *176*, 4701–4728. [[CrossRef](#)]
27. Cichostępski, K.; Kwietniak, A.; Dec, J. Verification of bright spots in the presence of thin beds by AVO and spectral analysis in Miocene sediments of Carpathian Foredeep. *Acta Geophys.* **2019**, *67*, 1731–1745. [[CrossRef](#)]
28. Pelton, J.R. Near-surface seismology: Surface-based methods. In *Near-Surface Geophysics*; Butler, D., Ed.; Society of Exploration Geophysicists: Tulsa, OK, USA, 2005. [[CrossRef](#)]
29. Sheehan, J.R.; Doll, W.E.; Mandell, W.A. An Evaluation of Methods and Available Software for Seismic Refraction Tomography Analysis. *J. Environ. Eng. Geophys.* **2005**, *10*, 21–34. [[CrossRef](#)]
30. Bery, A.A.; Saad, R. Correlation of Seismic P-Wave Velocities with Engineering Parameters (N Value and Rock Quality) for Tropical Environmental Study. *Int. J. Geosci.* **2012**, *3*, 749–757. [[CrossRef](#)]
31. Avalos, E.B.; Malone, D.H.; Peterson, E.W.; Anderson, W.P.; Gehrels, R.W. Two-dimensional seismic refraction tomography of a buried bedrock valley at Hallsands beach, Devon, United Kingdom. *Environ. Geosci.* **2016**, *23*, 179–193. [[CrossRef](#)]
32. Umor, M.R.; Arifin, M.H.; Muda, N. The Seismic Refraction Survey to Determine the Depth of Bedrock at the Damansara Area for Horizontal Directional Drilling Method Application. *Appl. Sci. Innov. Res.* **2019**, *3*, 123–132. [[CrossRef](#)]
33. Herlambang, N.; Riyanto, A. Determination of bedrock depth in Universitas Indonesia using the seismic refraction method. *IOP Conf. Ser. Earth Environ. Sci.* **2021**, *846*, 012016. [[CrossRef](#)]
34. Grelle, G.; Guadagno, F.M. Seismic refraction methodology for groundwater level determination: “Water seismic index”. *J. Appl. Geophys.* **2009**, *68*, 301–320. [[CrossRef](#)]
35. Xayavong, V.; Vu, M.D.; Nguyen, D.A.; Vu, T.M.; Chung, D.A.; Pham, L.T.; Eldosouky, A.M. Application of the Electrical Resistivity Tomography and Seismic Refraction Methods for groundwater Investigation in Savannakhet Province, Laos. *Front. Sci. Res. Technol.* **2022**, *3*, 62–69. [[CrossRef](#)]
36. Zainal, M.; Munir, B.; Abakar, M.; Yanis, M.; Muhni, A. Characterization of Landslide geometry using Seismic Refraction Tomography in the GayoLues, Indonesia. *J. Phys. Its Appl.* **2021**, *3*, 148–154. [[CrossRef](#)]
37. Imani, P.; El-Raouf, A.A.; Tian, G. Landslide investigation using Seismic Refraction Tomography method: A review. *Ann. Geophys.* **2021**, *64*, SE657. [[CrossRef](#)]
38. MacGregor, F.; Fell, R.; Mostyn, G.R.; Hocking, G.; McNally, G. The estimation of rock rippability. *Q. J. Eng. Geol.* **1994**, *27*, 123–144. [[CrossRef](#)]
39. Ismail, N.A.; Saad, R.; Nawawi, M.; Nordiana, M.M.; Ismail, N.H.; Mohamad, E.T. Identification of Rippability and Bedrock Depth Using Seismic Refraction. *AIP Conf. Proc.* **2010**, *1325*, 137–139. [[CrossRef](#)]

40. Ikard, S.J.; Rittgers, J.; Revil, A.; Mooney, M. Geophysical Investigation of Seepage Beneath an Earthen Dam. *Ground Water* **2014**, *53*, 238–250. [[CrossRef](#)] [[PubMed](#)]
41. Birkenmajer, K. Geologia Pienin. *Monogr. Pienińskie* **2017**, *3*, 5–66.
42. Adelinet, M.; Domínguez, C.; Fortin, J.; Violette, S. Seismic-refraction field experiments on Galapagos Islands: A quantitative tool for hydrogeology. *J. Appl. Geophys.* **2018**, *148*, 139–151. [[CrossRef](#)]
43. Olona, J.; Pulgar, J.A.; Fernández-Viejo, G.; López-Fernández, C.; González-Cortina, J.M. Weathering variations in a granitic massif and related geotechnical properties through seismic and electrical resistivity methods. *Near Surf. Geophys.* **2010**, *8*, 585–599. [[CrossRef](#)]
44. Zhang, J.; Toksöz, M.N. Nonlinear refraction travelttime tomography. *Geophysics* **1998**, *63*, 1726–1737. [[CrossRef](#)]
45. White, D.J. Two-dimensional seismic refraction tomography. *Geophy. J.* **1989**, *97*, 223–245. [[CrossRef](#)]
46. Aki, K.; Richards, P. *Quantitative Seismology. Theory and Methods*; Freeman: San Francisco, CA, USA, 1980.
47. Yilmaz, Ö. *Seismic Data Analysis*; Society of Exploration Geophysicists: Tulsa, OK, USA, 2001.
48. Everett, M.E. *Near-Surface Applied Geophysics*; Cambridge University Press: Cambridge, UK, 2013.
49. Guterch, A.; Grad, M.; Keller, G.R.; Posgay, K.; Vozár, J.; Špičák, A.; Brückl, E.; Hajnal, Z.; Thybo, H.; Selvi, O. Celebration 2000 seismic experiment. *Stud. Geophysica Geod.* **2003**, *47*, 659–669. [[CrossRef](#)]
50. Staniszewska, D.; Litwosz, T.; Pachuta, A.; Próchniewicz, D.; Szpunar, R. Geodynamic studies in the Pieniny Klippen Belt in 2004–2020. *Artif. Satell.* **2023**, *58*, 88–104. [[CrossRef](#)]
51. Czarnecka, K. Uwarunkowania strukturalne współczesnych ruchów tektonicznych pienińskiego pasa skałkowego w rejonie Czorsztyna. *Przegląd Geol.* **1986**, *10*, 556–560.
52. Walo, J.; Próchniewicz, D.; Olszak, T.; Pachuta, A.; Andrasik, E.; Szpunar, R. Geodynamic studies in the Pieniny Klippen Belt in 2004–2015. *Acta Geodyn. Geomater.* **2016**, *13*, 351–362. [[CrossRef](#)]
53. Lefeld, J.; Gaździcki, A.; Iwanow, A.; Krajewski, K. Jurassic and Cretaceous lithostratigraphic units of the Tatra Mts. *Stud. Geol. Pol.* **1985**, *84*, 1–86.

**Disclaimer/Publisher’s Note:** The statements, opinions and data contained in all publications are solely those of the individual author(s) and contributor(s) and not of MDPI and/or the editor(s). MDPI and/or the editor(s) disclaim responsibility for any injury to people or property resulting from any ideas, methods, instructions or products referred to in the content.